Influence of Stator Structure on Vibration of Switched Reluctance Motor

Kyung-Ho Ha, Young-Kyoun Kim, Geun-Ho Lee and Jung-Pyo Hong

Abstract - This paper deals with the influence of the various stator structures in a Switched Reluctance Motor (SRM) on the vibration behaviors. The stator part in SRMs produces most vibrations. Therefore, the geometric design of the stator is necessary to reduce the vibration. The free and forced vibrations for four different stator yoke structures are analyzed by the electromagnetic and structural Finite Element Method (FEM). Then vibration stator structure that offers less is proposed. The modal analysis results of a tested motor are compared with measurements.

Keywords – finite element method, forced vibration, free vibration, stator yoke, and switched reluctance motor

1. Introduction

In recent years, interest in Switched Reluctance Motor (SRM) drives has grown due to their simple and rugged construction, high efficiency, high power density, and lifetime. However, high levels of torque ripple and acoustic noise are the main drawbacks of SRM drives in many applications.

The interaction of electromagnetic forces and the mechanical structure of the SRM is the major cause of the noise and vibration [1,2]. To reduce the vibration, existing research focuses on either the drive strategies or the geometric design. The former approach offers smoothing or current shaping, switch angle control, and duty cycle according to the control mode [3]. The second approach, which is used in this study, deals with the mechanical design related to vibration behavior, in particular the geometric design of the stator considering the magnetic force wave [4,5,6].

The SRM is excited by large radial forces acting on opposite poles, which deform the stator into an oval. This vibration motion is most important when the harmonic frequency of the electrical excitation pattern coincides with the natural frequency of the stator. Therefore, the vibration behavior coupled with electromagnetic forces, natural frequencies, and mode shapes of the stator must be predicted.

The forced vibration of the stator is subjected to the electromagnetic force, which can be obtained by the frequency domain method or the time domain method [5]. The latter determines the dynamic response as a function of time in transient state and is useful for revealing the link between acoustic noise, stator vibration, and the current in the phase winding [3,5,6]. The modal analysis determines the vibration characteristic under a free structure of the stator, such as the natural frequencies or the mode shapes. The above analysis can be used at the design stage to avoid excessive vibration and hence reduce the noise generated.

Four stator structures modified from a common SRM with six poles on the round stator are used in this work: a round stator, a hexagon/round stator, and two hexagon stators. To propose a stator structure that is robust to vibration due to the magnetic force, the influence of the four models on vibration behavior is analyzed by the structural and electromagnetic FEM.

Initially, the effects of each model on the vibration modes and the corresponding natural frequencies of the SRM stator are compared via the modal analysis. The electromagnetic FEM is applied to the SRM magnetic structure to obtain the radial forces. Finally, this paper presents the forced vibration of the stator, when the radial magnetic force is applied at the surface of two opposite stator poles. The dynamic response in the time domain is used for analyzing the forced vibration.

This research is performed to propose a new stator structure with less vibration under the same magnetic force.

2. Computation Models of Stator Vibration

The analysis models are a SRM with 3-phase that has six stator poles and four rotor poles. Fig.1 presents the cross section of four stator structures examined in the structural FEA. All the models shown in Fig. 1 have about 5520 hexahedron elements used for 3D modeling of a solid structure. The element is defined by eight nodes having three degrees of freedom at each node.

Table 1 presents the measured mechanical properties needed for analysis of mechanical structure.

Manuscript received: Nov. 5, 2001 accepted : Aug. 1, 2002

K. H. Ha, Y. K. Kim and G. H. Lee are presently pursuing the Ph. D. degree in the Department of Electrical Engineering at Changwon National University, Changwon, Kyungnam, 641-773, Korea. (e-mail: haroom@netian.com, ensigma@hitel.net, lgh700@korea.com)

J. P. Hong is with the Department of Electrical Engineering at Changwon National University, Changwon, 641-773, Kyungnam, Korea(e-mail:jphong@sarim.changwon.ac.kr)

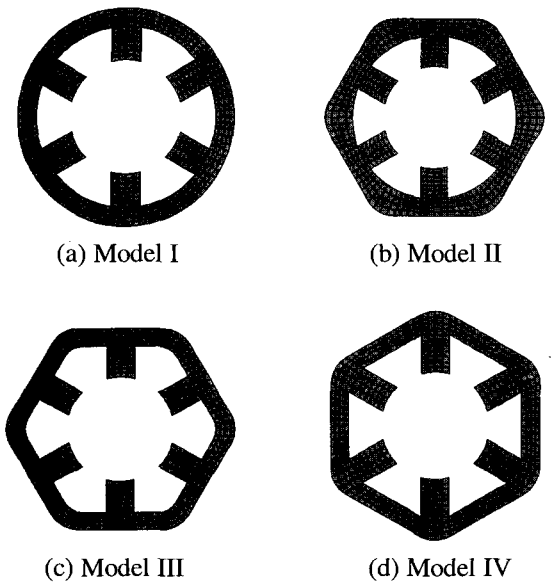

(a) Model I (b) Model II

(c) Model III (d) Model IV

Fig. 1 Four different structures of stator and mesh generation

Table 1 Mechanical Material Property

Young's modulus	Mass density of core	Poisson's ratio
205(Gpa)	7800(kg/m^3)	0.25

The stator yoke design of Models II, III and IV is based on Model I with the round stator.

- Model I: The round stator is a common cylinder configuration, which is the tested motor in this paper.
- Model II: The stator yoke's exterior is hexagonal and its interior is circular (hexagon/round stator).
- Model III: The stator yoke has a hexagon shape and the poles are positioned in the middle of each side.
- Model IV: The stator yoke is hexagonal and the poles are positioned at each corner.

The stator structure for each model is formed with a stack length, pole width, yoke thickness, and inner radius equal to that of the round stator.

3. Magnetic and Structural Analysis

3.1 Magnetic Force Calculation

For magnetic field analysis considering the nonlinear inductance profile of the SRM, the governing equation with vector potential is:

$$\nabla \times (\frac{1}{\mu} \nabla \times A) = J_0 \tag{1}$$

After equation (1) is coupled with the voltage equation, the system matrix is obtained by time difference schemes. The Maxwell stress tensor from the magnetic field analysis is used to obtain the exciting force acting on the stator. The electromagnetic force applied on the pole face of the stator core in the radial direction is evaluated by equation (2). The force density p between the stator core and air is represented as [2]:

$$p = \frac{1}{\mu_0}[(\mathbf{n} \cdot \mathbf{B})\mathbf{B} - \frac{1}{2} B^2 \mathbf{n}] \tag{2}$$

where $\mathbf{n}$ is the direction of the normal unit vector on the pole face and $\mathbf{B}$ is the flux density solved by electromagnetic FEA.

3.2 Modal Analysis

The vibration equation for an undamped system is based on the principle of Hamilton. The modal solution can be carried out using the stator model without fixed points.

$$[\mathbf{M}]\{\ddot{x}\} + [\mathbf{K}]\{\ddot{x}\} = \{0\} \tag{3}$$

where x is the vector of node displacement, and [**M**] and [**K**] are the global mass matrix and stiffness matrix.

The solution of free vibration will be a harmonic of the form

$$\{x(t)\} = e^{\omega_i t}\{\Phi\}_i \tag{4}$$

where $\{\Phi\}_i$ is an eigenvector representing the mode shape of the ith natural frequency, and ω_i is the ith natural frequency.

Thus, equation (3) leads to the eigenvalue problem

$$([\mathbf{K}] - \omega_i^2[\mathbf{M}])\{\Phi\}e^{\omega_i t} = \{0\} \tag{5}$$

A nontrivial solution of the set of equation (5) is possible only if the determinant coefficient vanishes.

$$\left|[\mathbf{K}] - \omega_i^2[\mathbf{M}]\right| = 0 \tag{6}$$

Equation (5) is solved for up to n value of ω^2.

3.3 Force Vibration Analysis

When the timing varying force is applied at a point or surface on the stator structure, the forced vibration pattern is examined by using the mode superposition method. To characterize the response of the structure with the dynamic load F, the response equation for the n modes to be used in the modal analysis is as follows. The response as a function of time is obtained by the solution of equation (7) [4,6].

$$[\mathbf{M}]\sum_{i=1}^{n}\{\Phi_i\}\ddot{y}_i(t) + [\mathbf{C}]\sum_{i=1}^{n}\{\Phi_i\}\dot{y}_i(t) + [\mathbf{K}]\sum_{i=1}^{n}\{\Phi_i\}y_i(t) = \{F(t)\} \tag{7}$$

where y_i is response, $\{\Phi_i\}$ is the mode shape factor of mode i, and $\{F(t)\}$ is the forcing term including the magnetic force.

4. Modal Analysis

Fig. 2 shows the frequency response function of Model I measured by experimental modal testing. This signal presents the transfer functions as a function of frequency,

while the impulsive excitation pulse is applied at several points of the structure. The peak points shown in Fig. 2 indicate the natural frequencies of the stator.

Table 2 shows the comparison of the natural frequencies of the four models via theoretical modal analysis. From the comparison of results for Model I, the relative error of the first natural frequency is 0.96%; the experimental natural frequency agrees with that calculated by FEM. The difference between calculation and experiment in high frequency is due to the lamination stack.

Fig. 3 presents the first two vibration modes according to the stator geometry. The mode shape characteristics of each model are similar as oval, triangular, and square with the increase of natural frequency. There is a gradual increase of the sides of a polygon with ascending natural frequency.

The oval mode given in (a1), (b1), (c1), (d1) of Fig. 3 may be excited by the electromagnetic symmetries due to the excitation pattern of the 6/4 SRM. These modes are main components of the acoustic noise. Among the oval modes, Model II (hexagon/round stator) creates the smallest nodal displacement. Then, the oval modes of each model are different. The frequency corresponding to Fig. 3(b1) becomes 1854Hz and the natural frequency of Fig. 3(c1) and Fig. 3(d1) decrease to 1375Hz and 1415Hz, respectively. With the help of these frequencies, the driver can determine the chopping frequency range for avoiding the vibration in the oval modes. (a2), (b2), (c2) and (d2) of Fig.3, the mode of the lamination stack in which the adjacent lamination would move against each other causes three-dimensional bending and torsion deformation. The bending mode cannot be vibrated in normal operation.

5. Forced Vibration

5.1 Magnetic Radial Force

Magnetic and elastic phenomena are assumed to be weakly coupled: the elastic deformation is small and consequently does not influence magnetic field distribution.

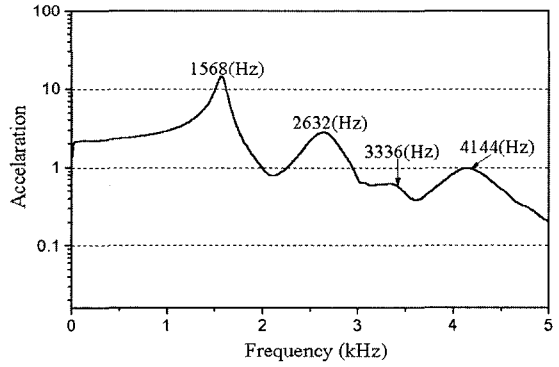

Fig. 2 Frequency response function for Model I obtained by experimental modal analysis

Table 2 Mechanical Material Property

Mode	Model I		Model II	Model III	Model IV
	FEM	Exp.			
1	1553	1568	1854	1379	1415
2	2819	2632	3236	2617	2617
3	3655	3336	4578	3093	3381
4	4567	4144	4979	4272	4035

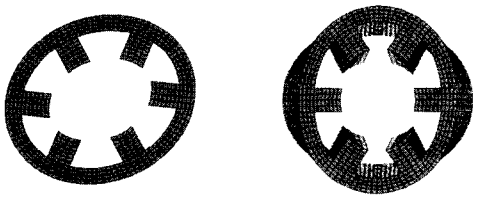

(a1) Mode at 1553Hz (Model I) (a2) Mode at 2819Hz (Model I)

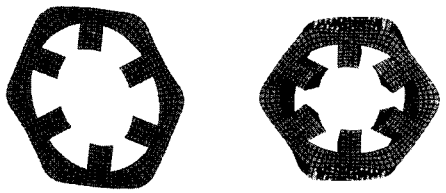

(b1) Mode at 1854Hz (Model II) (b2) Mode at 3236Hz (Model II)

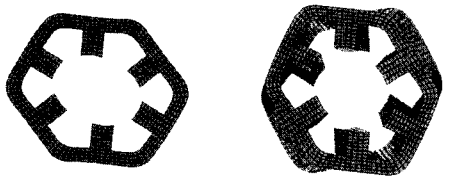

(c1) Mode at 1379Hz (Model III) (c2) Mode at 2617Hz (Model III)

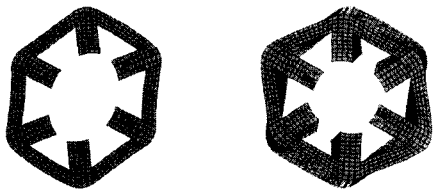

(d1) Mode at 1415Hz (Model IV) (d2) Mode at 2617Hz (Model IV)

Fig. 3 The fist two vibration modes corresponding to natural frequencies of SRM stator for four models

Fig. 4 shows the instantaneous global radial magnetic forces acting on the surface of the stator pole in Model I as a function of time. This result is obtained by the electromagnetic FEM by time stepping when only one phase on the opposite pole is excited. A period of the radial magnetic force for one phase excitation is 7.5(msec) at a speed of 2000(rpm). The maximum force is about 1.33(kN) just before the phase is turned off at 2.4(msec).

All the models produce almost the same radial force because the stator geometric dimension of each model except the stator yoke geometry is kept unchanged. The magnetic characteristics for each model, such as flux path, flux density and core loss, are almost identical.

5.2 Dynamic Response of Stator

As the calculated force wave is similar to a triangle wave, the approximate triangle wave to simplify the analysis is used to investigate the forced vibration in each model.

For the forced vibration of the stator, the displacement of a selected point A, as shown in Fig. 5, is observed while the radial force function is applied at the surface of two opposite stator poles. The dynamic response is analyzed by the structural FEM on the assumption that the damping for each model is ignored.

The displacements in the y-axis for each model are plotted as a function of time in Fig. 6. From this result, the displacement increases gradually up to 2.4(msec), above which it oscillates periodically. The structure moves into the stator center to reach a maximum displacement before the current is commuted and the stator moves back toward its original state and then oscillates as a damped vibration. As a result, a significant vibration is generated when the current in the phase winding is turned off because of the rapid change of the radial force. The maximum displacement for each model is displaying Fig. 6. The hexagon/round stator, Model II, shows the smallest displacement in the four models and is far superior in vibration reduction to the round stator and the hexagon stator. This result is the same nodal displacement of the oval mode predicted by the modal analysis.

In the hexagon/round stator, the thickness of the stator yoke at the corner increases the stiffness so that it is possible to suppress the deformation due to the radial force applied on the opposite poles. To further reduce the stator vibration, the hexagon/round model is selected to reinforce the strength in the stator pole corners and an appropriate fillet radius is determined from the dynamic response. From the analysis results, we determine the appropriate fillet radius is 5.0(mm) considering the manufacturing and motor performance.

Fig. 7 shows the comparison of the dynamic response between the test model and improved model. This result shows that the hexagon/round stator with the fillet radius produces less vibration than the test model. The configuration of the improved model is shown in Fig. 8.

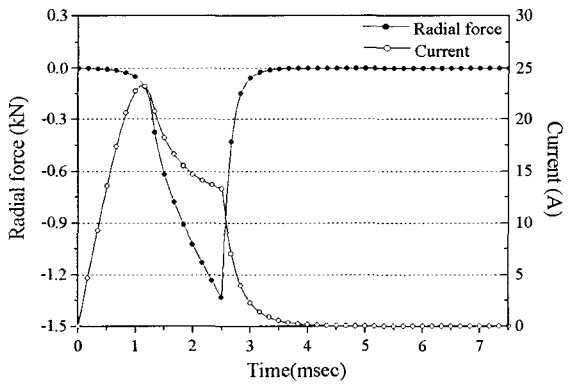

Fig. 4 Radial force as a function of time

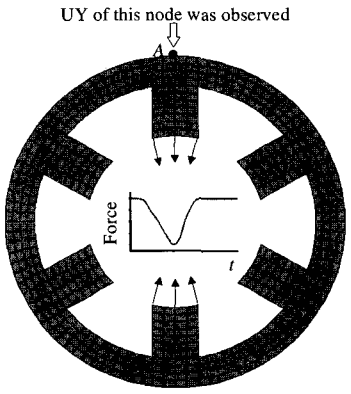

Fig. 5 Observing point for displacement calculation due to electromagnetic force

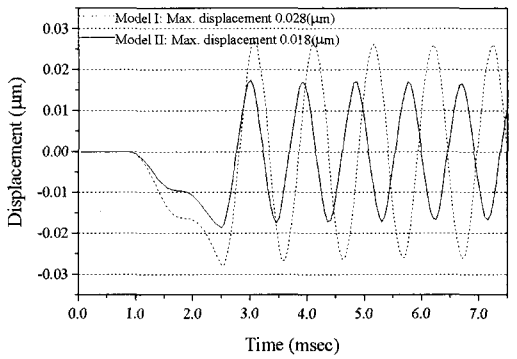

(a) Models I and II

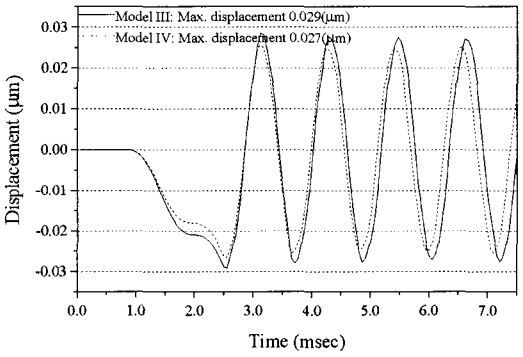

(b) Models III and IV

Fig. 6 Dynamic response of each stator due to the radial force applied to two opposite poles in time domain

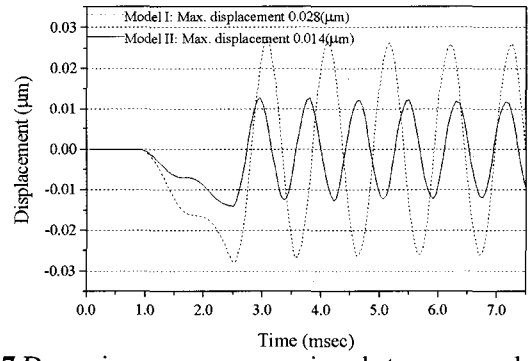

Fig. 7 Dynamic response comparison between round stator (Model I) and the hexagon/round stator (Model II) when the force with triangle wave is applied

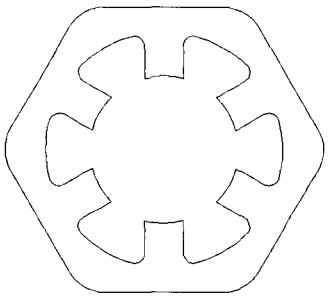

Fig. 8 Configuration of the proposed hexagon-round stator with the fillet at the pole corner for vibration reduction due to electromagnetic force

6. Conclusions

The free vibration and the forced vibration for the four stator structures in a 6/4 SRM are investigated by using structural and electromagnetic FEM and the analysis results are compared. The results of the study present the dominant mode shapes and resonance frequencies related to the radial force motion. In addition, the dynamic response of the stator is examined and the resulting deformation is analyzed. The proposed hexagon/round stator with the fillet radius produces less vibration than a common round stator in the 6/4 SRM.

References

[1] R. S. Colby, F. M. Mottier, and T. J. E. Miller, "Vibration modes and acoustic noise in a four-phase switched reluctance motor," *IEEE Trans. on Industrial Application*, vol. 32, pp. 1357-1364, November/ December, 1996.

[2] C. G. C. Neves *et al.*, "Vibration behavior of switched reluctance motors by simulation and experimental procedures," *IEEE Trans. on Magnetics*, vol. 34, pp. 3158-3136, September 1998.

[3] C. Pollock and C. Y. Wu, "Acoustic noise cancellation techniques for switched reluctance drives," *IEEE Trans. on Industrial Application*, vol. 33, pp. 477-484, March/April 1997.

[4] C. Picod, M. Besbes, and M. Gabsi, "Influence of stator geometry upon vibratory behaviour and electromagnetic performance of switched reluctance motors," *IEE Proc. Electric Power Application*, vol. 145, pp. 462-468, September 1998.

[5] P. Pillay and W. Cai, "An investigation into vibration in switched reluctance motors," *IEEE Trans. on Industrial Application*, vol. 353, pp. 589-596, 1999.

[6] A. Strassis and A. M. Michaelides, "The design of low vibration doubly salient motors," *Electric Machines and Power Systems*, vol. 27, pp. 967-981, 1999.

Kyung-Ho Ha was born in 1972. He received the B.S. and M.S. Degrees from Changwon National University, Changwon, Korea. He is presently pursuing the Ph.D. degree in the Dept. of Electrical Engineering at Changwon National University. His research interests include design of electric machines, numerical analysis of electromagnetics, and motor vibration.

Young-Kyoun Kim was born in 1971. He received the B.S. and M.S. Degrees from Changwon National University, Changwon, Korea. He is currently working toward the Ph.D. degree in Dept. of Electrical Engineering at Changwon National University. His research interests include design of electric machine, numerical analysis of electromagnetics, optimizations, and tolerance analysis.

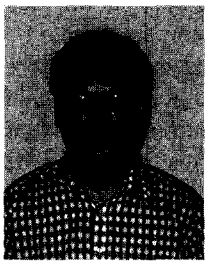

Geun-Ho Lee was born in 1969. He received the B.S. and M.S. Degrees from Hanyang University, Korea. From 1994 to 2002, he worked as senior research engineer at LG-OTIS. He is presently pursuing the Ph.D. degree in the Dept. of Electrical Engineering at Changwon National University. Since 2002, he has been working with Namhae College as an assistant professor. His research interests include design of electric machines, motor drivers, and motor vibration.

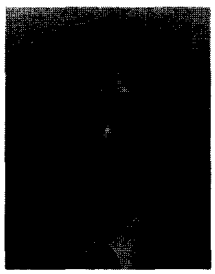

Jung-Pyo Hong was born in 1959. He received the B.S., M.S., and Ph.D. degrees from Hanyang University, Seoul, Korea. From 1992 to 1995, he was employed by LG Precision Co., Ltd., as an associate research engineer. From 1990 to 1992, he was employed by Samsung Electric Co., Ltd., as a senior research engineer. Since 1996, he has been an associate professor in the Department of Electrical Engineering at Changwon National University, Changwon, Korea. His research interests are design of electrical machines, optimizations, coupled problem, and numerical analysis of electromagnetics.